Floris, I.; Madrigal-Madrigal, J.; Sales Maicas, S.; Calderón García, PA.; Adam, JM. (2020). Twisting measurement and compensation of optical shape sensor based on spun multicore fiber. Mechanical Systems and Signal Processing. 140:1-9. https://doi.org/10.1016/j.ymssp.2020.106700

Twisting measurement and compensation of Optical Shape Sensor based on Spun Multicore Fiber

Ignazio Floris[a,b], Javier Madrigal[b], Salvador Sales[a], Pedro A. Calderón [b], Jose M. Adam[b*]

[a]*ITEAM , Universitat Politècnica de València, Camino de Vera s/n, Valencia, 46022, Spain*
[b]*ICITECH, Universitat Politècnica de València, Camino de Vera s/n, Valencia, 46022, Spain*

Abstract

This study presents a novel method for twisting compensation in optical shape sensing and first reports on twisting sensing by using Fiber Bragg Gratings (FBG) inscribed in a spun Multicore Fiber (MCF). A simple approach, based on Saint-Venant's Torsion Theory for homogeneous circular cylinders, was developed to calculate the fiber twisting from the longitudinal strain sensed in the cores and reconstruct three-dimensional shape taking into account and compensating the twisting, by enhancing the mathematical formulation of the previous approaches. Then, a 44mm-long pre-twisted fiber optic shape sensor was produced in the Institute for Telecommunications and Multimedia Applications (iTEAM) of the UPV, by writing four FBGs in a spun multicore fiber (diameter of 125.1 μm) with a pre-twisting of 64.9 rotation/meter. Finally, a series of experiments were performed to validate the method and evaluate the sensor performance. The outcomes of the experiments, perfectly in accordance with the theory, prove the elastic behavior of the sensor, even at high levels of deformation. Moreover, the proposed Spun-MCF-based Shape Sensor resulted able to measure twisting with a sensitivity of 0.23 pm/° and accuracy of 4.81° within a wide dynamic range of ± 270° (± 6136.4°/m). These new results can notably enhance the accuracy of fiber optic shape sensors and lead to the design of new fiber geometries and sensors.

Keywords *Spun Multicore Fiber; Twisted Multicore Fiber; Optical Shape Sensing;: Twisting Sensing; Optical Fiber Sensor; Distributed Sensing*

1. Introduction

Optical Fiber Sensors (OFS) have undergone a tremendous expansion over the last few decades in several different fields [1], such as engineering [2,3], industrial [4], medical [5], chemical [6,7] and biological [8,9]. The principal reasons behind this substantial growth are their considerable advantages over their electrical counterparts, including compactness, lightweight, electrically passive operation, resistance to harsh environments, and multiplexing capabilities. Besides OFSs have an inherent capability to sense a variety of measurands (as defined by [10]) in continuous development, such as strain [11,12], temperature [7], moisture [13], vibrations [14], chemical agents [9], and many others [15], using the optical fiber itself as a sensor.

One of the current frontier of the fiber-optic sensing technologies is shape sensing [16], which has been an area of great interest for many researchers and consists in the possibility to dynamically track position and shape of an optical fiber. Fiber Optic Shape Sensors (FOSS) consist of optical Multicore Fibers (MCF) (or sometimes multi-fiber cables, with the same section geometry but larger

* Corresponding author.
E-mail address: joadmar@upv.es (J.M. Adam)

core spacing) capable of sensing multidimensional curvature along the sensor's length, by comparing the longitudinal strain detected in different cores, and, hence, reconstructing shape [17].

Since curvature sensing using Fiber Bragg Gratings (FBG) inscribed in different cores of a MCF was first reported almost 20 years ago [18], a lot of progress has been made in this new branch. The two-dimensional shape of a multicore fiber was estimated based on distributed strain measurement [19,20]. An innovative approach for the three-dimensional shape reconstruction of a multicore optical fiber based on the numerical integration a set of Frenet-Serret equations was proposed by Moore et al. [21]. Fiber-optic shape sensing based on FBGs written in a MCF was employed in catheters, needles and minimally invasive surgery systems [5,22,23]. Tunnel monitoring was performed using multicore fiber displacement sensor [24]. Barrera et al. demonstrated a multicore optical fiber shape sensors suitable for use under gamma radiation [25].

Regrettably, due to the high flexibility, FOSSs are subject to twisting, in addition to bending and longitudinal strain. The twisting notably reduces the shape sensors' accuracy, causing significant uncertainty in the bending direction determination, when performing 3D shape sensing. Notwithstanding the vast amount of research conducted on shape sensing, this problem has not been addressed yet in an adequate manner. Tan et al. developed a torsion sensor based on inter-core mode coupling by tapering a multicore seven-core fiber [27]. Notwithstanding the innovation of this approach, it cannot be employed for shape sensing, since the fiber structure becomes inhomogeneous due to the tapering. Askins et al. first investigated the twisting of optical fibers using a tether fiber [26]. Despite its remarkable novelty, such research is not representative of the overwhelming majority of fiber optic shape sensors, consisting of MCF, and does not provide any information about the behavior of these sensors at high levels of twisting deformation, since only analyzed a limited dynamic range of twisting rotation, between ±600°/m. Twisting measurement using MCF is an extremely arduous task due to the littleness of the state of strain generated, as a result of the small core spacing. In order to overcome this limit, the multicore fiber could be pre-twisted to increase the twisting sensibility. In this respect, recent progresses in fabrication techniques have made possible the manufacturing of spun/twisted multicore fiber with very small spin pitch, 20mm (50 turn/m) [28] and even 15.4 mm (64.9 turn/m) [29,30], although their performance have not been investigated in depth. Nevertheless, an in-depth study focused on the performance of this new special multicore fiber is still missing.

The present work shows an innovative method to compensate the twisting of FOSSs and, thereby, enhances the accuracy in 3D shape reconstruction in presence of fiber twisting, by employing a spun multicore fiber (also called twisted multicore fiber), with one of the most used geometry for sensing applications: the seven-core fiber. The novelty of this research comes from: 1) the development of new and simple mathematical approach to calculate the twisting of multicore fiber based on the Saint-Venant's Torsion Theory for homogeneous circular cylinders; 2) the enhancement of one of the most used approaches for three-dimensional shape reconstruction in order to take into account the fiber twisting and automatically compensate it; 3) an experimental study carried out to successfully corroborate the mathematical approach and to evaluate the performance of optical shape sensor manufactured employing an innovative multicore spun fiber. Therewith, this research first demonstrates twisting sensing based on spun MCF shape sensor and illustrates the strong influence of the core spacing and spin pitch on the accuracy of pre-twisted multicore sensor in twisting sensing, laying the foundation for the design of new fiber geometries and new sensors.

2. Shape sensing with twisting compensation

This section illustrates an innovative approach, based on the Saint-Venant's Torsion Theory for homogeneous circular cylinders, to calculated the multicore fiber twisting from the longitudinal

strain of sensed in fiber cores and presents an enhancement of the method, proposed by Moore and Rogge [21], in order to reconstruct shape in presence of fiber twisting using spun MCF.

2.1. Twisting sensing

An optical fiber, subject to pure torsion/external twisting, which must not be confused with the geometric torsion τ, can be studied as a circular cylinder that has one fixed end and the other rotates of an angle θ. Hypothesizing that the fiber has perfectly elastic behavior, plane sections remain plane, radii remain straight and cross sections remain plane and circular, it is possible to apply the Saint-Venant's Torsion Theory for homogeneous circular cylinders [31]. Thereby, the sensor is in a state of pure shear and the shear strain γ in an element of the sensor is given by Eq. (1).

$$\gamma = r\frac{d\theta}{ds} \tag{1}$$

where r is the radial distance of the element from the sensor axis and $d\theta/ds$ represents the rate of change of the angle of twisting. Since every cross section has the same radius and is subjected to the same torque, the angle $\theta(s)$ varies linearly between extremities and $d\theta/ds$ is constant. Furthermore, the shear strain varies linearly with r, from zero at the centerline to a peak value at the free surface.

To calculate the longitudinal strain in a core, distant r from the axis, it can be considered that the cores, initially straight, become circular helices ($d\theta/ds$ is constant) due to twisting, as shown in Fig. 1.

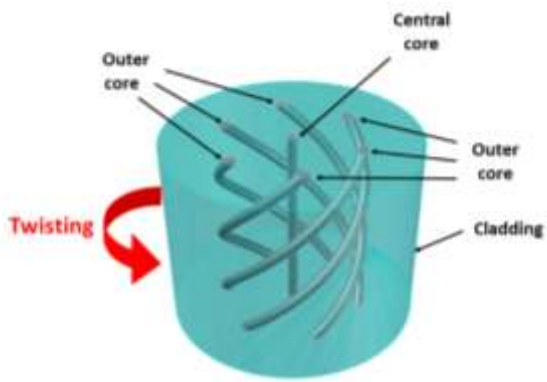

Fig. 1. Twisted multicore seven-core fiber.

The length of a core in a twisted multicore fiber can be calculated as the length of a circular helix by Eq. (2):

$$x = \sqrt{h^2 + r^2\theta^2} \tag{2}$$

where x is the length of the core, h is the length of the sensor and r is the distance of the core from the sensor axis and the reciprocal distance between the closest outer cores, generally called core-to-core spacing or, simply, core spacing.

Thus, the longitudinal strain of the cores due to twisting can be calculated from the definition of strain (Eq. (3).

$$\varepsilon = \frac{x-h}{h} = \frac{\sqrt{h^2+r^2\theta^2}-h}{h} \tag{3}$$

As it can be noticed from (3), the longitudinal strain is remarkably influenced by the core spacing, length of the sensor and angle of twisting being the same. Moreover, the central core is not affected by the twisting, since its axis coincides with the sensor axis. Fig. 2 shows the variation of longitudinal strain due to twisting of an outer core in relation to core spacing and twisting angle per meter.

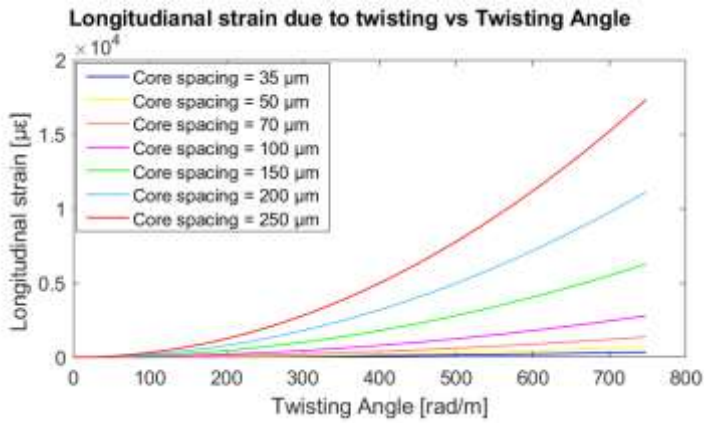

Fig. 2. Longitudinal strain due to twisting in relation to core spacing and twisting angle.

When performing three-dimensional shape sensing, the sensor is not only subject to twisting but also to bending, axial strain and thermal expansion. In this case, the component of strain due to twisting, ε_{twist}, can be calculated as defined in Eq. (4).

$$\varepsilon_{twist} = \frac{\sum_{i=1}^{n} \varepsilon_i^{outer}}{(n-1)} - \varepsilon_{central} \tag{4}$$

where ε_i^{outer} is the strain of the *i-th* outer core, $\varepsilon_{central}$ is the strain of the central core and n is the number of cores.

Eq. (4) is valid for the seven-core section geometry studied in this research and for all the section geometries with a central core and several outer cores, equidistant form the sensor axis and with equal angular spacing between them, such as the four-core and five-core section geometries with, respectively, 3 and 4 outer cores and 1 central core.

Finally, the angle of twisting can be calculated from the strain sensed in the cores, combining (3) and (4), as defined in Eq. (5).

$$\theta = \sqrt{\frac{h^2\varepsilon_{twist}^2+2h^2\varepsilon_{twist}}{r^2}} \tag{5}$$

It has to be pointed out that the longitudinal strain generated in the outer cores by the twisting of a non-twisted multicore fiber does not depend on direction of rotation. In other words, the twisting of a non-twisted MCF of an angle $-\theta$ or $+\theta$ always produces a positive longitudinal strain variation of the outer cores, making impossible to distinguish the sense of twisting rotation from the strain detected in the cores. To avoid this problem, a spun/pre-twisted MCF has to be used. Thereby, a twisting rotation in the direction concordant with the pre-twisting rotation produces an elongation

of the outer cores, while, a twisting in the opposite direction, produces shortening. Furthermore, using a spun multicore fiber is also possible to increase the sensor sensitivity to twisting, as shown in Fig. 3 for a multicore fiber with core spacing of 35 µm.

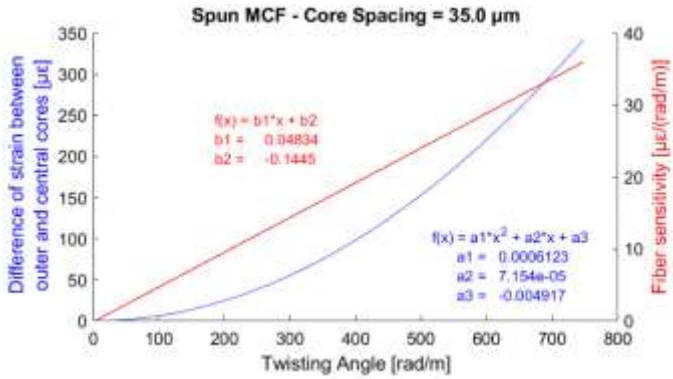

Fig. 3. Longitudinal strain due to twisting and fiber sensitivity to twisting in relation twisting angle for a multicore fiber with core spacing of 35 µm.

2.2. Shape reconstruction with twisting compensation

Fiber optic shape sensors are OFSs with multiple cores and embedded strain sensors. Under the Kirchhoff's rod hypotheses [32], the longitudinal strain of the fiber and the three-dimensional curvature along fiber's length can be calculated from the strain sensed by the cores, using the Eqs. (6), (7), and (8) [17,33–35].

$$\begin{cases} \varepsilon_{long} = \sum_{i=1}^{n} \varepsilon_i / n \\ \kappa_x = \sum_{i=1}^{n} x_i \varepsilon_i / \sum_{i=1}^{n} x_i^2 \\ \kappa_y = \sum_{i=1}^{n} y_i \varepsilon_i / \sum_{i=1}^{n} y_i^2 \end{cases} \tag{6}$$

$$|\kappa| = \sqrt{\kappa_x^2 + \kappa_y^2} \tag{7}$$

$$\alpha = \tan^{-1}(\kappa_x / \kappa_y) \tag{8}$$

where ε_{long} is the longitudinal strain, κ_x, κ_y and $|\kappa|$ are the two components of curvature and the curvature magnitude, x_i, y_i and ε_i are, respectively, the coordinates and the strain of the *i-th* core, and α is the bending direction angle, which defines the bending direction.

Once calculated the fiber twisting along the fiber, its effects can be compensated by applying the superposition principle and correcting the bending direction angle in each instrumented section according to Eq. (9).

$$\alpha' = \alpha - \theta \tag{9}$$

where α' is the compensated bending direction angle.

Hence, by mean of interpolation or curve fitting [21,36], the functions of curvature, $\kappa(s)$, and torsion, $\tau(s)$, along the fiber can be determined respectively from curvature and from the bending direction angle (see Eqs. (9) and (10)).

$$\tau(s) = \frac{d\alpha'}{ds} \tag{10}$$

Finally, the 3D shape of the sensors can be obtained through numerical integration of the Frenet-Serret formulas (Eq. (11))[21]:

$$\begin{bmatrix} \boldsymbol{T}' \\ \boldsymbol{N}' \\ \boldsymbol{B}' \end{bmatrix} = \begin{bmatrix} 0 & \kappa & 0 \\ -\kappa & 0 & \tau \\ 0 & -\tau & 0 \end{bmatrix} \begin{bmatrix} \boldsymbol{T} \\ \boldsymbol{N} \\ \boldsymbol{B} \end{bmatrix} \tag{11}$$

where $\boldsymbol{T}$, $\boldsymbol{N}$ and $\boldsymbol{B}$ are, respectively, the tangent, normal and binormal vectors.

It is worth noting that the approach here presented is valid for several optical strain sensing technologies, including FBGs, Brillouin and Rayleigh scattering, and for different number of cores and sensor geometries, including multi-fiber shape sensors and multicore fiber shape sensors. Nonetheless, this research is only focused on multicore fiber shape sensors, since they are the most used [5,17,21,23], thanks to their compactness, ease of handling and availability, being employed for communication purposes.

It is also worth pointing out that, when it is valid the assumption of absence or negligibility of external twisting/torsion, its compensation can be omitted, for instance when the shape sensor is fastened to a rigid support, although this would limit its handiness and compactness and restrict its possible applications. Whereas, in general cases, if not compensated, the twisting leads to remarkable uncertainty in the determination of the bending direction and drastically reduces the accuracy of the sensor in performing three-dimensional shape sensing.

3. Spun fiber optic shape sensor fabrication

A pre-twisted fiber optic shape sensor was produced in the Institute of Telecommunications and Multimedia Applications (iTEAM) of the *Universitat Politècnica de València* (UPV) by writing Fiber Bragg Gratings in a spun 7-core multicore fiber (see Fig. 1) with a spin pitch of 15.4 mm (64.9 rotation/meter), manufactured and provided by FIBERCORE Ltd. [29,37]. The fiber had seven single-mode cores (mode field diameter of 6.4 μm and numerical aperture of 0.2) with doubly symmetric configuration (60º of angular spacing and core spacing of 35 μm) and a cladding diameter of 125.1 μm.

The spun multicore fiber was hydrogen-loaded for 14 days at ambient temperature and at a pressure of 20 bars with the purpose of improving the photosensitivity. Afterward, four FBG were inscribed in a 44mm long portion of the fiber by means of a 244 nm CW frequency-doubled argon-ion laser with 60 mW output power using the phase-mask method [38]. The size of the laser beam was adjusted in order to reach all cores and the inscription was carried out simultaneously in the seven cores.

4. Experimental setup

Fig. 4 illustrates the experimental setup. The pre-twisted fiber optic shape sensor was fastened with two fiber rotators, situated at 44 mm distance from one another and assembled on multi-axis stages for nano-positioning.

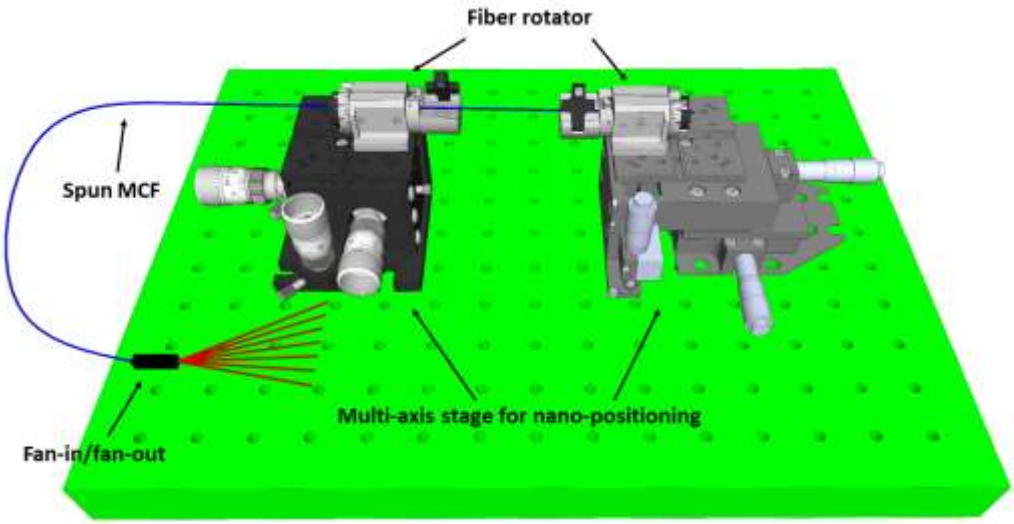

Fig. 4. Experimental setup.

First, the left fiber rotator was turned from 0° to 270° in the direction coherent with the pre-twisting and, then, moved back to the initial position. This sense of rotation is defined positive because stretches the outer cores. Thereafter, the right rotator was rotated between 0° and -270° in the negative sense of rotation, which shortens the outer cores. The sensor was interrogated by using a Static Optical Sensing Interrogator (sm125) combined with a Channel Multiplexer (sm041) (Micron Optics).

5. Results and discussion

The pre-twisted multicore shape sensor was placed on the fiber rotators and the core spectra were recorded. Then, the FBG peaks were tracked during the experiments and their wavelength shifts were calculated and converted into strain, dividing them by a gauge factor value of 1.2 pm/με, obtained from several tensile tests and in accordance with the literature [39]. The spectra of the seven cores are plotted in Fig. 5.

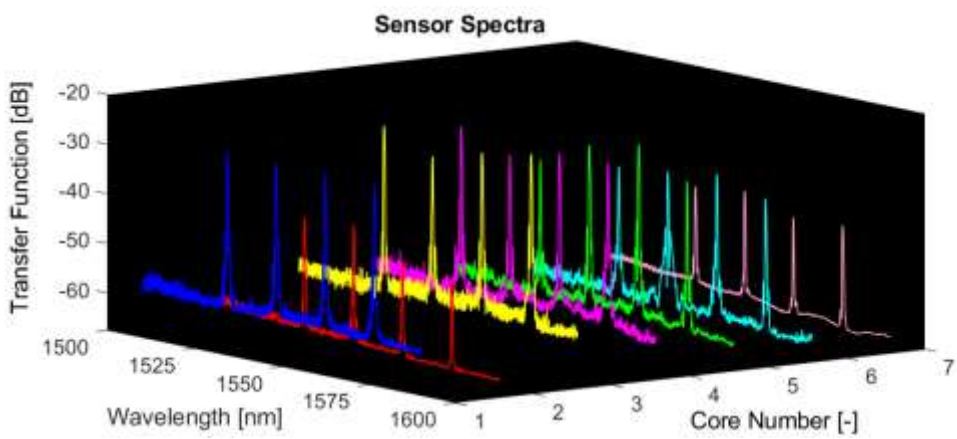

Fig. 5. Core spectra (the central core is the core number 1, while the cores from 2 to 7 are outer cores ordered in clockwise direction).

With the aim of evaluating the accuracy of the sensor in measuring twisting, the strain of the cores was tracked, while the sensor was being twisted in the positive and negative sense of rotation, considering as positive the direction of rotation that elongates the outer cores. The values of twisting angle applied during the experiments and the resulting values of strain of the outer core due to twisting, calculated in accordance with the theoretical approach presented in Subsection 2.1, are listed in Table 1.

Table 1. Inputs and outputs of the experiments according to the theoretical approach presented in Subsection 2.1.

Test nº	Twisting rotation [°]	Twisting and pre-twisting rotation [rad]	Fiber spin pitch [mm]	Outer cores strain variation due to twisting and pre-twisting [με]	Outer cores strain variation due to twisting [με]
0	0	17.95	15.40	101.95	0.00
1	5	18.04	15.33	102.95	0.99
2	10	18.13	15.25	103.95	1.99
3	15	18.21	15.18	104.95	3.00
4	20	18.30	15.11	105.96	4.00
5	30	18.48	14.96	107.99	6.03
6	40	18.65	14.82	110.04	8.08
7	50	18.82	14.69	112.11	10.15
8	60	19.00	14.55	114.19	12.24
9	90	19.52	14.16	120.57	18.62
10	120	20.05	13.79	127.13	25.18
11	150	20.57	13.44	133.86	31.90
12	180	21.09	13.11	140.76	38.80
13	210	21.62	12.79	147.83	45.88
14	240	22.14	12.49	155.08	53.12
15	270	22.66	12.20	162.50	60.55
0	0	17.95	15.40	101.95	0.00
1	-5	17.86	15.48	100.96	-0.99
2	-10	17.78	15.55	99.98	-1.97
3	-15	17.69	15.63	99.00	-2.95
4	-20	17.60	15.71	98.03	-3.93
5	-30	17.43	15.86	96.09	-5.86
6	-40	17.25	16.02	94.18	-7.78
7	-50	17.08	16.19	92.28	-9.67
8	-60	16.90	16.35	90.41	-11.55
9	-90	16.38	16.88	84.89	-17.06
10	-120	15.86	17.43	79.55	-22.40
11	-150	15.33	18.03	74.39	-27.57
12	-180	14.81	18.67	69.39	-32.56
13	-210	14.29	19.35	64.57	-37.38
14	-240	13.76	20.09	59.93	-42.03
15	-270	13.24	20.88	55.45	-46.50

Fig. 6 shows the comparison between the predicted values and the outcomes of the experiments. The experiments results are perfectly consistent with the outputs of the theoretical approach, proving that the hypotheses of the Saint-Venant's Torsion Theory hold in this problem and that the fiber has elastic behavior even at high values of deformation. The sensor was able to detect the fiber twisting with an average sensitivity of 0.23 pm/° and an accuracy of 4.81° within a wide dynamic range of ± 270° (± 6136.4°/m), while the a maximum error was of 13.53°.

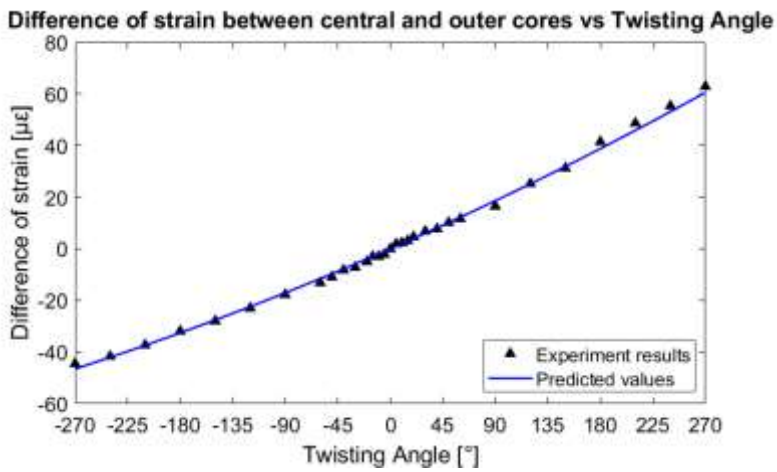

Fig. 6. Comparison between predicted values and experiment outcomes.

It has to be highlighted that, even though the fiber has a perfectly elastic behavior, the relationship between strain and twisting angle is a nonlinear and monotonically increasing function, as shown by Eq. (5) and Fig. 6. In the light of this, the sensitivity of the sensor to twisting as well as its accuracy grow with the increasing twisting and pre-twisting rotations (decreasing spin pitch). Consequently, the performance of the sensor can be improved by increasing the pre-twisting rotation, in addition to increasing the core spacing (see Eq. (9)). Moreover, it has to be emphasized that no temperature compensation was necessary, since the distance between the cores of the spun multicore fiber is extremely small (35 μm) and, therefore, it can be assumed that the temperature is constant in the section.

6. Conclusions

This paper reports on experimental study carried out to investigate the performance of an innovative spun-MCF-based fiber optic shape sensor in twisting sensing and presents a simple method enhance the accuracy in shape sensing, by compensating the fiber twisting.

The outcomes of the experiments, perfectly consistent with the theory, first demonstrate that optical shape sensors based on spun multicore fiber are efficiently able to sense twisting and prove the perfectly elastic behavior of the fiber, even at high levels of twisting deformation, assumption underpinning the Saint-Venant's Torsion Theory. Altogether, the sensor, long 44 mm, was able to sense twisting with a sensitivity of 0.23 pm/° and accuracy of 4.81° within a wide dynamic range of ± 270° (± 6136.4°/m).

In addition, this research, by defining the influence of core spacing and spin pitch on the accuracy of pre-twisted fiber optic shape sensor in twisting sensing, lays the foundations for the design of a new generation of optical shape sensors.

Acknowledgments

This work was carried out within the ITN-FINESSE framework, funded by the European Union's Horizon 2020 Research and Innovation Program under the Marie Sklodowska-Curie Action Grant Agreement N° 722509. It was also supported by the Ministry of Economy and Competitiveness of Spain under DIMENSION TEC2017-88029-R.

References

[1] D. Tosi, E. Schena, C. Molardi, S. Korganbayev, Fiber optic sensors for sub-centimeter spatially resolved measurements: Review and biomedical applications, Opt. Fiber Technol. 43 (2018) 6–19. doi:10.1016/j.yofte.2018.03.007.

[2] J. He, Z. Zhou, O. Jinping, Optic fiber sensor-based smart bridge cable with functionality of self-sensing, Mech. Syst. Signal Process. 35 (2013) 84–94. doi:10.1016/j.ymssp.2012.08.022.

[3] N. Roveri, A. Carcaterra, A. Sestieri, Real-time monitoring of railway infrastructures using fibre Bragg grating sensors, Mech. Syst. Signal Process. 60–61 (2015) 14–28. doi:10.1016/j.ymssp.2015.01.003.

[4] H. Alian, S. Konforty, U. Ben-Simon, R. Klein, M. Tur, J. Bortman, Bearing fault detection and fault size estimation using fiber-optic sensors, Mech. Syst. Signal Process. 120 (2019) 392–407. doi:10.1016/j.ymssp.2018.10.035.

[5] A. Beisenova, A. Issatayeva, D. Tosi, C. Molardi, Fiber-Optic Distributed Strain Sensing Needle for Real-Time Guidance in Epidural Anesthesia, IEEE Sens. J. 18 (2018) 8034–8044. doi:10.1109/JSEN.2018.2865220.

[6] A. Sultangazin, J. Kusmangaliyev, A. Aitkulov, D. Akilbekova, M. Olivero, D. Tosi, Design of a Smartphone Plastic Optical Fiber Chemical Sensor for Hydrogen Sulfide Detection, IEEE Sens. J. 17 (2017) 6935–6940. doi:10.1109/JSEN.2017.2752717.

[7] J. Madrigal, D. Barrera, S. Sales, Refractive Index and Temperature Sensing Using Inter-Core Crosstalk in Multicore Fibers, J. Light. Technol. 37 (2019) 4703–4709. doi:10.1109/JLT.2019.2917629.

[8] M. Piestrzyńska, M. Dominik, K. Kosiel, M. Janczuk-Richter, K. Szot-Karpińska, E. Brzozowska, L. Shao, J. Niedziółka-Jonsson, W.J. Bock, M. Śmietana, Ultrasensitive tantalum oxide nano-coated long-period gratings for detection of various biological targets, Biosens. Bioelectron. 133 (2019) 8–15. doi:10.1016/j.bios.2019.03.006.

[9] Y. Zhao, X. Zhou, X. Li, Y. Zhang, Review on the graphene based optical fiber chemical and biological sensors, Sensors Actuators B Chem. 231 (2016) 324–340. doi:10.1016/j.snb.2016.03.026.

[10] I. Gertsbakh, Measurement Theory for Engineers, in: Meas. Theory Eng., Springer Berlin Heidelberg, Berlin, Heidelberg, 2003. doi:10.1007/978-3-662-08583-7_1.

[11] P. Li, Z. Zhang, J. Zhang, Simultaneously identifying displacement and strain flexibility using long-gauge fiber optic sensors, Mech. Syst. Signal Process. 114 (2019) 54–67. doi:10.1016/j.ymssp.2018.05.005.

[12] Z. Zhou, W. Liu, Y. Huang, H. Wang, H. Jianping, M. Huang, O. Jinping, Optical fiber Bragg grating sensor assembly for 3D strain monitoring and its case study in highway pavement, Mech. Syst. Signal Process. 28 (2012) 36–49. doi:10.1016/j.ymssp.2011.10.003.

[13] M. Mieloszyk, W. Ostachowicz, Moisture contamination detection in adhesive bond using embedded FBG sensors, Mech. Syst. Signal Process. 84 (2017) 1–14. doi:10.1016/j.ymssp.2016.07.006.

[14] P.L. Fuhr, P.J. Kajenski, D.L. Kunkel, D.R. Huston, A subcarrier intensity modulated fiber optic sensor for structural vibration measurements, Mech. Syst. Signal Process. 7 (1993) 133–143. doi:10.1006/mssp.1993.1003.

[15] D. Zheng, Z. Cai, I. Floris, J. Madrigal, W. Pan, X. Zou, S. Sales, X.I.Z. Ou, S.A.S. Ales, Temperature-insensitive optical tilt sensor based on a single eccentric-core fiber Bragg grating, Opt. Lett. (n.d.). doi:10.1364/OL.99.099999.

[16] M. Amanzadeh, S.M. Aminossadati, M.S. Kizil, A.D. Rakić, Recent developments in fibre optic shape sensing, Meas. J. Int. Meas. Confed. 128 (2018) 119–137. doi:10.1016/j.measurement.2018.06.034.

[17] I. Floris, J. Madrigal, S. Sales, J.M. Adam, P.A. Calderón, Experimental study of the influence of FBG length on optical shape sensor performance, Opt. Lasers Eng. 126 (2020) 105878. doi:10.1016/j.optlaseng.2019.105878.

[18] M.J. Gander, W.N. MacPherson, R. McBride, J.D.C. Jones, L. Zhang, I. Bennion, P.M. Blanchard, J.G. Burnett, a H. Greenaway, Bend mesurement using Bragg gratings in multicore fibre, Electron. Lett. 36 (2000) 2–3.

[19] G.A. Miller, C.G. Askins, E.J. Friebele, Shape sensing using distributed fiber optic strain measurements, in: Second Eur. Work. Opt. Fibre Sensors, 2004: p. 528. doi:10.1117/12.566653.

[20] R.G. Duncan, M.E. Froggatt, S.T. Kreger, R.J. Seeley, D.K. Gifford, A.K. Sang, M.S. Wolfe, High-accuracy fiber-optic shape sensing, in: K.J. Peters (Ed.), 2007: p. 65301S. doi:10.1117/12.720914.

[21] J.P. Moore, M.D. Rogge, Shape sensing using multi-core fiber optic cable and parametric curve solutions, Opt. Express. 20 (2012) 2967. doi:10.1364/OE.20.002967.

[22] H. Moon, J. Jeong, S. Kang, K. Kim, Y.-W. Song, J. Kim, Fiber-Bragg-grating-based ultrathin shape sensors displaying single-channel sweeping for minimally invasive surgery, Opt. Lasers Eng. 59 (2014) 50–55. doi:10.1016/j.optlaseng.2014.03.005.

[23] F. Khan, A. Denasi, D. Barrera, J. Madrigal, S. Sales, S. Misra, Multi-core Optical Fibers with Bragg Gratings as Shape Sensor for Flexible Medical Instruments, IEEE Sens. J. PP (2019) 1–1. doi:10.1109/JSEN.2019.2905010.

[24] W.N. MacPherson, M. Silva-Lopez, J.S. Barton, a J. Moore, J.D.C. Jones, D. Zhao, L. Zhang, I. Bennion, N. Metje, D.N. Chapman, C.D.F. Rogers, Tunnel monitoring using multicore fibre displacement sensor, Meas. Sci. Technol. 17 (2006) 1180–1185. doi:10.1088/0957-0233/17/5/S41.

[25] D. Barrera, J. Madrigal, S. Delepine-Lesoille, S. Sales, Multicore optical fiber shape sensors suitable for use under gamma radiation, Opt. Express. 27 (2019) 29026. doi:10.1364/OE.27.029026.

[26] C.G. Askins, G.A. Miller, E.J. Friebele, Bend and Twist Sensing in a Multiple-Core Optical Fiber, in: OFC/NFOEC 2008 - 2008 Conf. Opt. Fiber Commun. Fiber Opt. Eng. Conf., IEEE, 2008: pp. 1–3. doi:10.1109/OFC.2008.4528404.

[27] F. Tan, Z. Liu, J. Tu, C. Yu, C. Lu, H.-Y. Tam, Torsion sensor based on inter-core mode coupling in seven-core fiber, Opt. Express. 26 (2018) 19835. doi:10.1364/oe.26.019835.

[28] P.S. Westbrook, K.S. Feder, T. Kremp, T.F. Taunay, E. Monberg, J. Kelliher, R. Ortiz, K. Bradley, K.S. Abedin, D. Au, G. Puc, Integrated optical fiber shape sensor modules based on twisted multicore fiber grating arrays, in: I. Gannot (Ed.), 2014: p. 89380H. doi:10.1117/12.2041775.

[29] L.J. Cooper, A.S. Webb, A. Gillooly, M. Hill, T. Read, P. Maton, J. Hankey, A. Bergonzo, Design and performance of multicore fiber optimized towards communications and sensing applications, in: S. Jiang, M.J.F. Digonnet (Eds.), Proc. SPIE - Int. Soc. Opt. Eng., 2015: p. 93590H. doi:10.1117/12.2076950.

[30] https://www.fibercore.com/product/multicore-fiber, https://www.fibercore.com/product/multicore-fiber, (n.d.).

[31] A.E.H. Love, A Treatise on the Mathematical Theory of Elasticity, 1st ed., Cambridge University Press, 1892. https://hal.archives-ouvertes.fr/hal-01307751.

[32] O.M. O'Reilly, Kirchhoff's Rod Theory, in: Model. Nonlinear Probl. Mech. Strings Rods Role Balanc. Laws, Springer International Publishing, Cham, 2017: pp. 187–268. doi:10.1007/978-3-319-50598-5_5.

[33] I. Floris, S. Sales, P.A. Calderón, J.M. Adam, Measurement uncertainty of multicore optical fiber sensors used to sense curvature and bending direction, Meas. J. Int. Meas. Confed. 132 (2019). doi:10.1016/j.measurement.2018.09.033.

[34] I. Floris, P.A. Calderón, S. Sales, J.M. Adam, Effects of core position uncertainty on optical shape sensor accuracy, Measurement. 139 (2019) 21–33. doi:10.1016/j.measurement.2019.03.031.

[35] I. Floris, J.M. Adam, P.A. Calderòn, S. Sales, Measurement uncertainty of 7-core multicore fiber shape sensors, in: K. Kalli, G. Brambilla, S.O. O'Keeffe (Eds.), Seventh Eur. Work. Opt. Fibre Sensors, SPIE, 2019: p. 22. doi:10.1117/12.2539421.

[36] S. Jäckle, J. Strehlow, S. Heldmann, Shape Sensing with Fiber Bragg Grating Sensors, in: H. Handels, T.M. Deserno, A. Maier, K.H. Maier-Hein, C. Palm, T. Tolxdorff (Eds.), Bild. Für Die Medizin 2019, Springer Fachmedien Wiesbaden, Wiesbaden, 2019: pp. 258–263. doi:10.1007/978-3-658-25326-4_58.

[37] https://www.fibercore.com/product/multicore-fiber, (n.d.).

[38] R. Kashyap, Fiber Bragg Gratings, 2nd Editio, Elsevier, 2010. https://www.elsevier.com/books/fiber-bragg-

gratings/978-0-12-372579-0.

[39] R.J. Black, D. Zare, L. Oblea, Y.-L. Park, B. Moslehi, C. Neslen, On the Gage Factor for Optical Fiber Grating Strain Gages, Proc. Soc. Adv. Mater. Process Eng. 52, 2008 (2008). http://www.cs.cmu.edu/~ylpark/publications/SAMPE_08.pdf.